A dynamical approach to modelling visuomotor activity: comparison between dorsal and ventral premotor cortices

Pedro Miguel Correia Pinto Sabido [1] pedro.pinto.sabido@gmail.com

Thesis to obtain the Master of Science degree in Biomedical Engineering

Supervised by: Peter Janssen [2] João Sanches [3]

28th November 2019

Abstract - Currently, intracortical BMIs rely almost exclusively on activity in the primary motor cortex. In many clinical conditions, however, this area is damaged or severely degenerated, which limits the restoration of movement to patients. The premotor and parietal cortices, responsible for coordinating the planning of motor commands through visuomotor integration, are, on the other hand, less often affected and, thus, may represent an alternative for BMI control. Recent research suggests that motor information can be extracted from the dynamical structure underlying neural trajectories in motor and premotor areas. The present work compares the adequacy of representing the neuronal activity in the dorsal (PMd) and ventral (PMv) premotor cortex of a rhesus monkey during a reach-to-grasp task with such a dynamical model. The results show very robust dynamical rotations in both areas in all epochs of the task, despite the low average response in PMv before movement onset. Furthermore, this project also seeks to investigate the usability and flexibility of a visuomotor BMI that uses the dynamical rotations of premotor neuronal populations to decode movement direction and onset. The decoding accuracy of both motor parameters was above chance level, with dynamical trajectories performing notoriously better than the combination of the spiking responses of all channels. This work suggests that a dynamical representation of premotor activity may yield satisfactory results for the control of a motor BMI in a discrete space.

Keywords - Visuomotor BMI, state-space modelling, neuronal dynamics, rotational dynamics in PMd and PMv, decoding of motor parameter.

1 INTRODUCTION

In many clinical conditions, characterised by limb amputation, spinal injury, damage (e.g. after a stroke) or severe degeneration (e.g. in amyotrophic lateral sclerosis) of primary motor cortex (M1) neurons, patients' mobility is compromised and so is their clinical rehabilitation. [1, 2] Naturally, the restoration of movement to patients with some level of motor impairment can have a determinant impact in their biopsychosocial adjustment. With that in mind, research in Brain-machine Interfaces (BMIs) has become an emergent field of research. Most major studies in humans, however, have been conducted with M1 inputs, an area that can be affected in some of the aforementioned clinical conditions. [1, 3] We propose visuomotor neuronal activity of the premotor areas as an alternative to M1 motor inputs.

1.1 Visuomotor encoding in the brain

Visuomotor skills describe the actions produced when visual and motor cortices work in concert. [4] In order to use these signals for BMI control, it is essential to understand how the representation of visual object properties transitions into intended motor acts, i.e. how the brain "sees" and analyses object location and shape to guide action.

The visual system is divided into a dorsal pathway, corresponding to the projections established from the primary visual cortex to several areas in the intraparietal sulcus (IPS) and a ventral stream, running from the primary visual cortex to the inferotemporal cortex (ITC). Several studies have suggested that the ventral stream is essential for processing object information for visual perception and object identification (replying to "what is the object?") and the dorsal stream plays a role in the processing of spatial information and object characteristics to guide actions (giving an answer to "where is the object and how does it look?"). [5–7]

The FARS model describes the anterior intraparietal area (AIP) as the first stage in the grasp programming process, where object-related information from the posterior intraparietal area (PIP) (dorsal stream) and object identification from the ITC (ventral stream) are integrated and a set of possible ways of grasping the object - called affordances - is computed. This information is passed on to ventral premotor area (PMv) (F5), where, given a set of constraints, only one grasp option is selected. These constraints include task information from pre-supplementary motor area (pre-SMA) (F6), working memory or behaviour inhibition from the prefrontal cortex (PFC) - which relies on object recognition in ITC -, and instruction stimuli from dorsal premotor area (PMd)

[1]Instituto Superior Técnico, Universidade de Lisboa and Faculty of Medicine, Katholieke Universiteit Leuven
[2]Department of Neuroscience and Faculty of Medicine, Katholieke Universiteit Leuven
[3]Bioengineering Department and Institute for Systems and Robotics, Instituto Superior Técnico, Universidade de Lisboa

(F2). In this last case, F2 is known to bias the selection of the grasp in tasks where the right grasp is conditional upon presentation of a stimulus. [6]

PMv (F5) neurons in nonhuman primates have been described to discharge during specific hand movements, namely holding, tearing, manipulating, and, most predominantly, grasping. [8] Moreover, neurons in this area have shown selectivity to the type of hand grip required (e.g. precision grip, finger prehension, or whole-hand grasping). [9] Several electrophysiological studies have also stressed the role of PMv (F5) neurons in visually-guided tasks, with particular responsibility in executing and monitoring the preshaping of the hand and the grasping of objects. [6, 10]

PMd, on the other hand, plays a more significant role in the planning of reaching actions by retrieving, retaining and integrating visuospatial information about both target and arm location. [10, 11] The activity in PMd has been reported to reflect the planning of several directional signals, when primates face multiple potential reaching actions. These signals are later eliminated when a subsequent nonspatial cue identifies the correct action. [10, 12]

Despite the strong influence that this dichotomy between reaching in PMd and grasping in PMv has had in neuroscientific research, researchers have suggested that this division is not absolute. In fact, Takashi et al. (2017) found grasping-tuned neurons in PMd, and neurons with a preference for reaching in PMv. [13] Nonetheless, both PMd and PMv use information about object characteristics and spatial organisation to drive the planning of motor behaviour, which suggests the potential of these premotor areas in BMI control. [10, 13–15]

1.2 Dynamical interpretation of visuomotor activity

Throughout the history of neuroscience research, there has been an undeniable interest in understanding how movement is generated in our brain. Two conflicting models have, since then, proposed possible interpretations of how neuronal responses instruct motion: the representational and the dynamical views.

The representational view explains the activity of single neurons as a function of movement parameters, supporting the premise that the individual motor cortical neurons encode many high-level or abstract movement features. [16, 17] The dynamical systems view, on the other hand, considers that individual neurons' responses are not a representation of meaningful variables, as the responses of individual neurons rarely match the electromyographic patterns. Instead, dynamical models can produce multiphasic electromyographic signals from the patterns of activity of population-level latent variables, and their internal dynamics. [17, 18]

Inspired by their observations that rhythmic muscle contraction in both a swimming leech and a walking monkey matched the oscillation frequency of cortical responses, Churchland et al. (2012) proposed treating neuronal responses as a dynamical system itself. They concluded that, if individual neurons have oscillatory activity, the overall population response should rotate with time. [16] In order to test this hypothesis, this team developed jPCA, a method that seeks linear combinations of principal components (obtained via Principal Component Analysis (PCA)) that capture the rotational structure of the dynamical trajectories in a population of neurons. [16] Indeed, not only were quasi-oscillatory neuronal responses found in a motor neuronal population during a reach-to-grasp task, but they even captured a large portion of the variance observed. [16, 17] This may come as a surprise, as the task itself is not rhythmic, but the rotational patterns were still present. [16]

Since then, many studies have reported that the rotational patterns underlying M1 and PMd trajectories during reach-to grasp tasks can describe the patterns of motor activity. [2,16,18] We evaluate the extent to which rotational dynamics are also present in the multi-unit activity (MUA) recorded in PMv (F5). Moreover, this work investigates the usability and flexibility of visuomotor dynamics for motor control by attempting to extract movement direction and movement onset from the activity in PMd.

2 METHODS

2.1 Electrophysiological recordings

The neuronal data used in the present work were recorded in one male rhesus monkey (*Macaca mulatta*, 8 kg). After training the subject in a reach-to-grasp task, a titanium head post was fixed to the subject's skull with dental acrylic and ceramic screws, and two 96-channel micro-electrode Utah arrays with 1.5-mm-long electrodes and an electrode spacing of 0.4 mm (Blackrock Microsystems, UT, USA) were implanted in the right dorsal premotor area F2, PMd, and the ventral premotor area F5c, PMv, contralaterally to the subject's working hand.

All channels were connected to digital headstages (Cereplex M, Blackrock Microsystems, UT, USA). The recordings were then sent to a Cerebus data acquisition system (Blackrock Microsystems, UT, USA) at a 30 kHz sampling frequency. A multiunit detection trigger was set to detect spikes in the neural activity, with a threshold of 95% of the maximum noise recorded for each individual channel.

The data were acquired in two distinct periods of time: in the first experiment only PMd was recorded, whereas in the second set of recordings PMd and PMv neurons were recorded simultaneously. The first set of data are used for decoding movement parameters, and the second recordings are used to compare the rotational structure in the two premotor areas.

All experimental protocols were approved by the ethical committee on animal experiments of KU Leuven and performed according to the *National Institute of Health's Guide for the Care and Use of Laboratory Animals* and the EU Directive 2010/63/EU.

2.2 Experimental paradigm

During experimental procedures, neuronal activity was recorded while the monkey sat upright in a primate chair with its head fixed. A custom-built object (15 cm diameter) containing three identical spheres (2.5 cm of diameter) was placed 34 cm in front of the monkey. A green LED in the centre of the large object indicated the go cue. Each sphere, positioned in an angle of 120° relative to the other two spheres, contained a blue LED used to signal the object to be grasped. In each task repetition (also referred to as a trial), the monkey was instructed to reach for and grasp one of the spheres in a pseudo-random order, while its neuronal activity was being recorded. Each sphere corresponded to a different experimental condition, as all spheres required a different reaching direction and, consequently, triggered different patterns of neuronal activity.

To start a trial, the monkey positioned its left hand on a hand-rest in complete darkness. Shortly after the start, the green LED lighted up and, after at least 500 ms of fixation on the green light, one blue LED went on (object onset), indicating which of the spheres the monkey had to pull. Simultaneously to the blue LED, an external light source illuminated the object from above. After a variable time, the green LED was turned off (go cue), instructing the monkey to reach for the cued object. The time interval between the instant when the monkey effectively released the hand-rest (lift hand) and pulled the sphere (pull object) could not exceed 1000 ms otherwise the trial was considered incorrect. A correctly-executed trial was rewarded with juice. The inter-trial interval was 1000 ms.

2.3 Data Processing

The recorded data corresponds to spike times of the MUA detected by each electrode. To obtain the spike rates at a given time point, the number of recorded spikes in a 20-ms bin centred in that instant was divided by the duration of the interval - hence the unit of spike/s. The rates were calculated every 10 ms, following the concept of a running average. The signal in each channel was normalised by subtraction of the average spike rate in a 300-ms interval recorded immediately before object onset - baseline activity. Additionally, the Peristimulus Time Histograms (PSTHs) were smoothed with a 24-ms Gaussian filter, in order to simulate temporal continuity.

2.4 jPCA: Representing rotational dynamics

A major concern in neuroscientific experiments is the organisation and visualisation of data. Each experiment may record from many channels, and the signal recorded in a channel varies with time and experimental condition, creating a high-dimensional state-space, which may be difficult to work with.

With the goal of facilitating structural exploration of neuronal data, the Churchland laboratory developed jPCA, a dynamical variant of PCA. The code for jPCA is available at `https://churchland.zuckermaninstitute.columbia.edu/`. While PCA finds direction of maximal variance, jPCA finds planes of significant rotational structure. [16] Although completely independent, these methods play complementary roles in this project, as PCA (with 6 principal components) was always applied before jPCA, ensuring that the rotational structure found could explain a considerable amount of data variance.

2.5 SVM: decoding movement parameters

The decoding of movement direction (task condition) and movement onset was performed with the MATLAB toolbox for Support Vector Machine (SVM). The training of this machine requires a set of labelled observations, each one characterised by various features. The set of observations was divided into two sets: a training set, that contained about 90% of the observations and was used to train the model, and a test set, constituted by the remaining 10%, that evaluated the performance of the new-found model.

When decoding movement direction (task condition), each trial was considered an observation. As such, jPCA was performed to find the six jPCA projections that captured the most rotational structure for all individual trials simultaneously, rather than the across-trial average for trials recorded under the same condition. For each observation, each instant in a jPCA projection was considered a feature. Similarly, when decoding with the PSTHs of all neurons instead of jPCA projections, each time instant in each channel was acknowledged as a feature.

For the purpose of decoding movement onset, each trial retrieved two observations: one sampled during a 300-ms-long interval preceding the lift of the hand (labelled 'Onset'), and another one sampled in the interval [50; 350] after object onset (labelled 'Not Onset'). The two groups were then joined, forming a set of observations with double the number of trials in the dataset. The feature design, with either jPCA projections or the spike rates of the entire neuronal ensemble, was similar to the analogous procedure described for decoding movement direction.

In both cases, the feature space was significantly reduced using the MATLAB function for feature selection, *sequentialfs*, following a 10-fold cross validation procedure. To train the algorithm, data dimensionality was raised using a *radial basis function* kernel, which was empirically found most suitable for the analyses carried out. In order to improve performance, the kernel scale and the box constraint were optimised each time the machine was trained. For each model, Mdl, trained with the selected features, the labels of the test set were predicted and the accuracy determined as the percentage of correct label predictions.

For a test of statistical significance, each set of decoding conditions (dataset, feature design and decoding interval, when decoding movement direction) was repeated 100 times with different training and test sets, generat-

ing a distribution of statistical parameters.

2.6 Material Specifications

All data were analysed using custom written Matlab scripts (MATLAB R2018b, Mathworks, MA, USA). The Matlab's Java Heap Memory preferences were set to 4.014 MB, and the scripts were run on a Precision 5820 Tower (Dell, TX, USA) with a 12-core 3.6 GHz processor, 16384 MB RAM and SSD.

3 RESULTS AND DISCUSSION

3.1 Rotational structure in PMd and PMv dynamics

The activity recorded in the studied premotor areas is, during the reach-to-grasp task, roughly characterised by a peak of PMd activity during the visual phase (while planning the reach movement), and a more intense PMv activity after the movement starts, to guide the hand towards the objects.

The spike rate of each recording channel can be used to create a 64-dimensional state-space, where each recorded channel represents one dimension. A possible state can, thus, be represented by a point with 64 coordinates. An additional dimension - time - can be included to create the concept of neuronal trajectory, which is nothing more than a temporal sequence of states. In an attempt to make processing of neuronal dynamical patterns less computationally burdensome, jPCA can be used to reduce data dimensionality and rotate the architecture of the states in state-space, revealing the already existing rotational structure.

We analysed the dynamical rotations of neuronal ensembles in both premotor areas in various epochs during the reach-to-grasp tasks, as described in table 1, in order to facilitate a structured comparison between the rotations and evaluate the performance of jPCA throughout the task. Although not all jPCA plots are included, in all datasets analysed and in both areas the neuronal trajectories were clearly less organised and overlapped much more before object onset (figs. 1(a) and 2(a)) as opposed to later epochs (figs. 1(b), 1(c), 2(b) and 2(c)).

Table 1: Intervals used in the comparative analysis of the rotational structure in PMd and PMv. The column «Align» defines the event to which the starting and ending points are relative: object onset (OO), go cue (GC), lift of the hand (LH) and grabbing the object (PO).

Interval	Start (ms)	End (ms)	Align
I. Before object onset	-300	0	OO
II. After object onset	100	400	OO
III. After go cue	50	350	GC
IV. During lift hand	-150	150	LH
V. During grab object	-200	100	GO

In general, PMd trajectories seemed to have slightly more distinct projections in the earlier epochs than PMv, which could be observed not only for the first jPCA plane but for all 3 jPCA planes analysed.

To assess the goodness of the fit of the constrained model, M_{skew}, to neuron populations in PMd and PMv, we can analyse the data variance capture by the jPCA planes, or use statistical measures, such as the coefficient of determination (CD) and the rotational goodness-of-fit ratio (RGR). The dynamical trajectories in both areas not only showed robust rotational patterns, but also captured a great part of data variance ($> 80\%$, fig. 3(a)) -

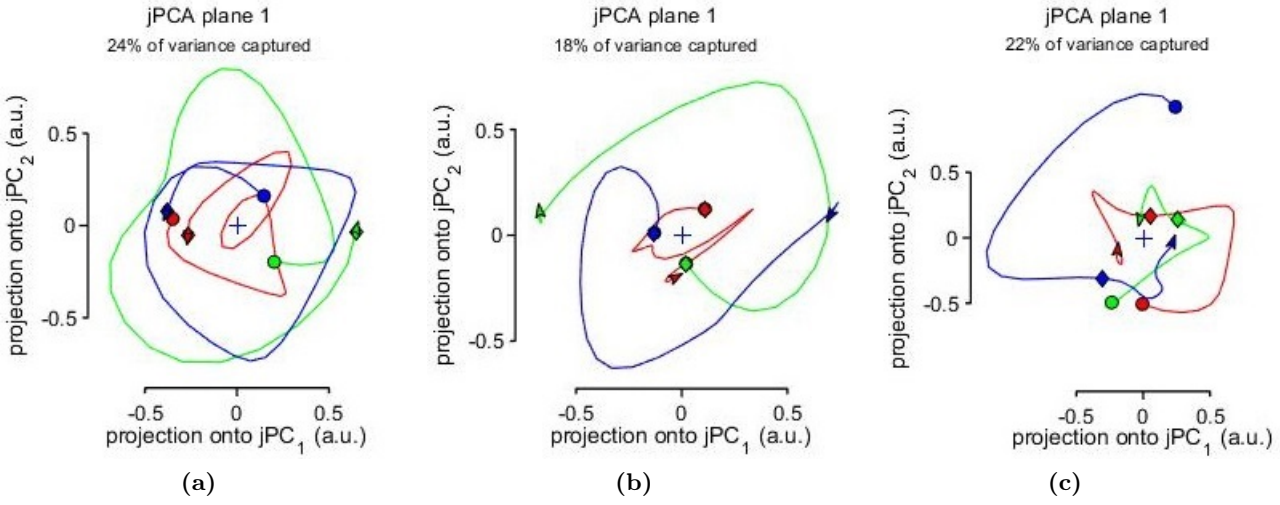

Figure 1: Projection of the multi-unit activity of a PMd neuronal population in monkey J3 onto the first jPCA plane. The plots in **(a)**-**(c)** described the activity in the intervals I, II and IV in table 1. The jPCA planes are found within a space defined by 6 principal components. Each trace represents the trajectory for condition 1 (in red), condition 2 (in green) and condition 3 (in blue). The circle and the arrow represent the starting and the end points of the analysis, respectively, and the diamond is plotted on the point corresponding to the event of alignment.

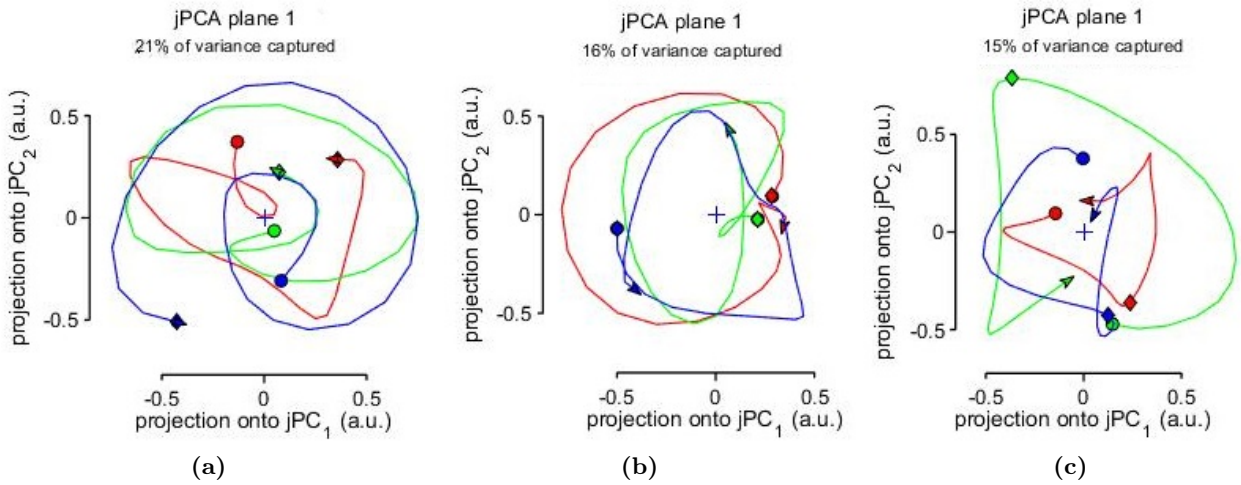

(a) **(b)** **(c)**

Figure 2: Projection of the multi-unit activity of a PMv neuronal population in monkey J3 onto the first jPCA plane. The plots in **(a)-(c)** described the activity in the intervals I, II and IV in table 1. The jPCA planes are found within a space defined by 6 principal components. Each trace represents the trajectory for condition 1 (in red), condition 2 (in green) and condition 3 (in blue). The circle and the arrow represent the starting and the end points of the analysis, respectively, and the diamond is plotted on the point corresponding to the event of alignment.

a substantial result given that we are representing 64-dimensional information in a 6-dimensional space. The CD, $R^2_{M_{skew}}$, expresses how well rotational dynamics predict the overall data behaviour. It is worth noting that the smaller the interval of analysis, the easier it is to fit a model to the neuronal behaviour, and, thus, the better this statistic. Regardless of that, the most important remark here is that the neuronal trajectories in both premotor areas seem to be equally well represented by rotational patterns (fig. 3(b)). The RGR, $R^2_{M_{skew}}/R^2_M$, is a useful measure to understand the fraction of neuronal linear dynamics that can be accurately represented with rotational structure, as opposed to a linear structure with expansions/contractions. For all datasets and intervals analysed, a considerable portion of the variance explained by linear dynamics was, in fact, captured by the rotations in the state-space (fig. 3(c)) in both areas.

A potential concern with the use of jPCA is that it may be sufficiently powerful to find rotational dynamics for any population with diversified and multiphasic responses. Furthermore, it is also sensible to analytically assess the extent to which rotational patterns may be found by chance, when responses are diverse and complex but do not correspond to actual neuronal dynamics.

A first evaluation, based on the analysis of Churchland et al. (2012), involves three shuffled controls that disrupt the deep structure of the data but conserve the data covariance. [16] These shuffled controls are built around the distinction between pre-stimulus phase and the stimulus-driven phase, divided at a time-point 100 ms after the object onset. In the first shuffled control, the stimulus-driven activity was time-inverted for one or two conditions randomly selected, preserving the continuity of the signals for each neuron. The second shuffled control is similar to the first but for all conditions. The third shuffled control consists in permuting the stimulus-driven activity of different conditions: the stimulus-driven activity of each condition is appended to the final firing rate of the pre-stimulus activity of a different condition, preserving the continuity of the signals for each neuron.

To efficiently quantify any loss of rotation strength, one can measure the angle from the neural state on a jPCA plane, X, to its derivative, $\dot{X}$: robust rotations should have positive angles with values close to $\pi/2$ *rad*, whereas linear trajectories result in angles near 0 *rad* and π *rad*. [16] For most datasets and both premotor areas, the original neuronal trajectories showed consistently more $\pi/2$ *rad* angles and a complete absence of $-\pi/2$ *rad* angles (which would imply finding clockwise rotations, which is not expected; data not shown), whereas shuffled data have more expansions (0 *rad* angles) and some clockwise and anticlockwise rotations. Both statistical measures, CD and RGR, assumed strictly better results for the original data ($R^2_{M_{skew}} \sim 60\%$ and $RGR \sim 90\%$ for all datasets and both premotor areas) when compared to the corresponding shuffled data ($R^2_{M_{skew}} \in [23; 65]\%$ and $RGR \in [44; 80]\%$, with shuffle 2 having the worst results, and shuffle 1 the best).

This control test does not consider that "random" variations in trajectories of individual conditions might be the reason why jPCA fits the neuronal activity in these datasets so well. To assess this possibility, the second test, inspired by the work of Lara et al. (2018), simulates a new neuronal population by altering the covariance of the original data. [19] A bootstrap is employed

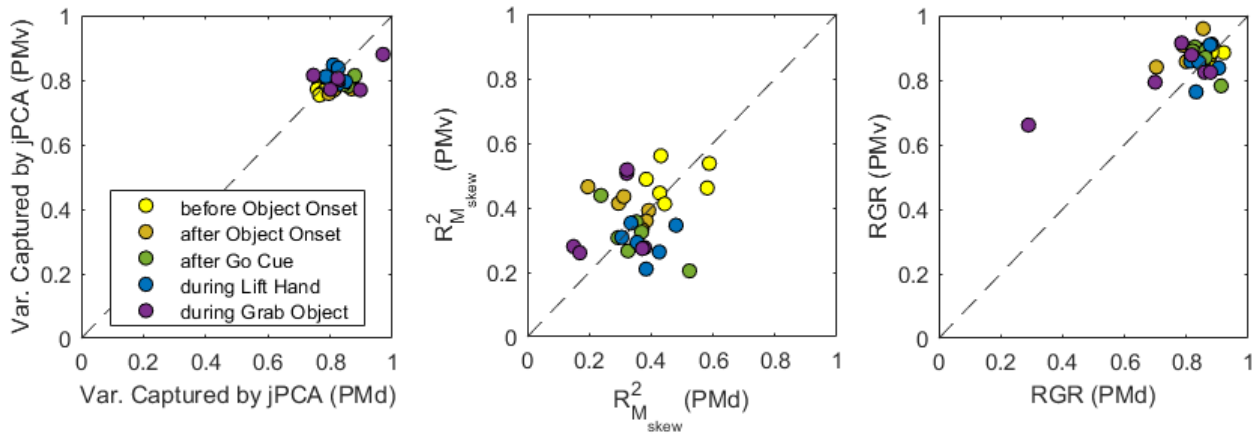

(a) **(b)** **(c)**

Figure 3: Comparison of the goodness of fit of the 3 jPCA planes calculated for the PMd and PMv populations recorded in datasets J1-J6 and for all intervals mentioned in table 1: **(a)** variance captured by the 6 jPCA projections, **(b)** coefficient of determination of the constrained system, $R^2_{M_{skew}}$, and **(c)** RGR. The model was calculated with the rank-6 matrices that capture dynamics in all 6 analysed dimensions.

in which each of the columns of X (each column is a jPCA component, where the rows are grouped in 3 sets, each set including the projection of the neuronal activity in a different condition) and $\dot{X}$ are modified to include 3 redrawn conditions, with replacement, from 3 columns, also with replacement. This process is repeated 1000 times for each dataset and epoch to provide a sampling distribution. We evaluated the probability of obtaining equal or better statistics in the bootstraps than those of the original data, and verified that the shuffling led to an overall loss of rotational structure, $R^2_{M_{skew}}$, and a loss of preponderance of rotations in the general linear dynamics, RGR, both with p-value < 0.05.

These results suggest that the overall MUA in these premotor areas is, indeed, very well described by rotational dynamics, which is no surprise in PMd, as various studies have already reported and evaluated jPCA in this context, but is, as far as we know, a novelty in PMv. [2, 16, 20]

3.2 Unravelling the neuronal code in PMd

The control of arm movement with a BMI requires the clear identification of the movement direction and the onset of the action. With this in mind, we attempted to give some practical meaning to the rotations of PMd neuronal trajectories, by decoding these two movement parameters from the jPCA projection in this area with an SVM. In both cases, the performance was evaluated in comparison to the results obtained when decoding with the PSTHs of each channel.

3.2.1 Decoding movement direction

For the purpose of decoding movement direction, rotational behaviour was analysed for the three intervals presented in table 2. The first interval serves as a negative control, as no distinction is expected between the neuronal activity associated to each condition before object onset. This is true for raw spike rates and for the jPCA projections.

Table 2: Intervals used in the decoding of movement direction. The column «Align» defines the event to which the starting and ending points are relative: object onset (OO) or lift of the hand (LH).

Interval	Start (ms)	End (ms)	Align
I. Before object onset	-300	0	OO
II. After object onset	50	350	OO
III. During lift hand	-50	250	LH

The experimental setup is designed so that each object (experimental condition) is shown as often as all the other objects. Thus, the chance level for randomly attributing the correct label to an observation in the test set is about 33%. This value is not rigorous, as each test set is not constrained to have a balanced number of observations with each label.

As expected, both feature designs yielded an average decoding accuracy distribution centred around the chance level for interval I (figs. 4(a) and 4(b)) – a result that validates the classification method, as observations are not correctly labelled more often than expected by chance. For the other two intervals, the accuracy was significantly above chance level, with average correctness ranging from 61 to 81% with jPCA projections and from 45 to 58% with the spike rates of the entire neuronal ensemble.

Our observations lead us to believe that trials underlying the same experimental condition are characterised by a certain neuronal trajectory. The minor variations caused by artefacts and noise are mostly lost due to dimensionality reduction and, thus, trials recorded under the same condition should span the state-space similarly.

Furthermore, there does not seem to exist any relation between the decoding performance in intervals 2 and 3 in either feature designs. This result suggests that the flow-field of the neuronal activity in the low-dimensional

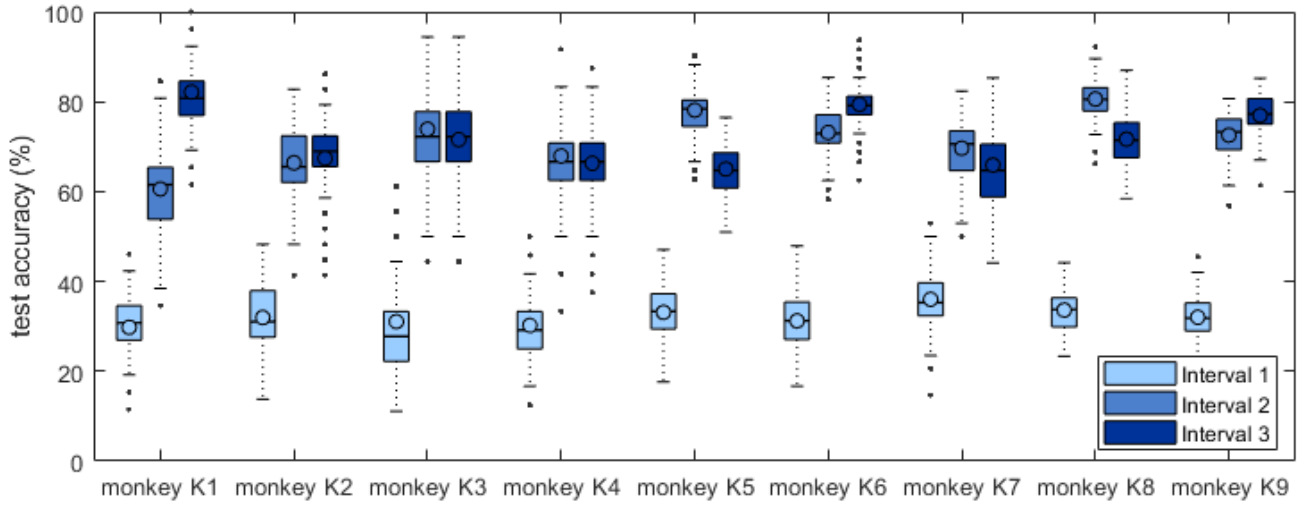

(a)

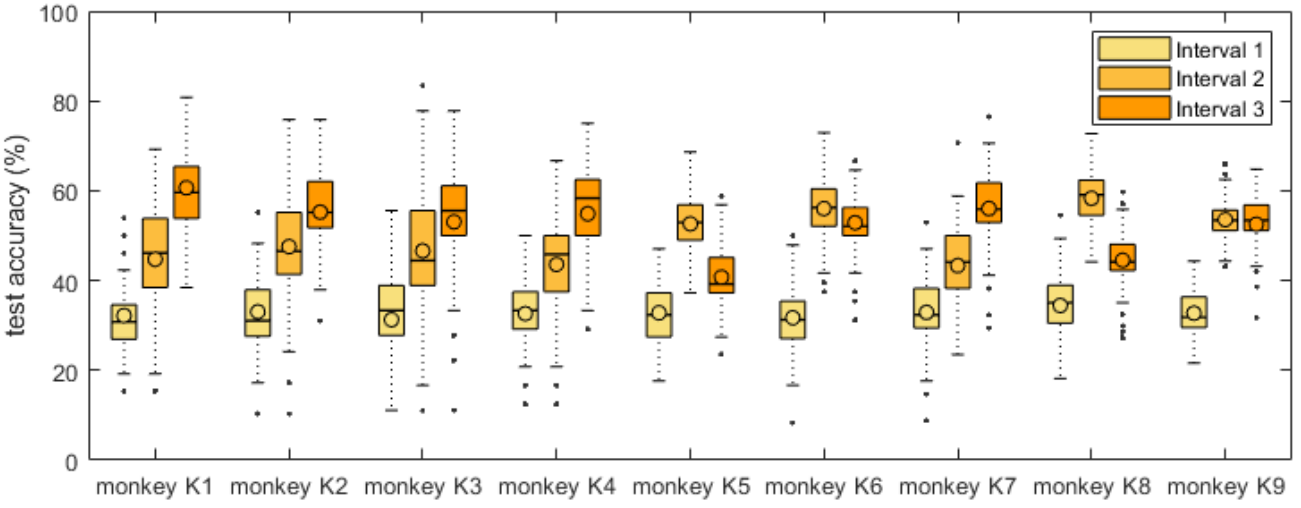

(b)

Figure 4: Accuracy of decoding movement direction with **(a)** jPCA projections versus **(b)** the trains of spike rates (PSTHs) of the entire neuronal ensemble. The decoding procedure was performed for datasets K1-9 for the time intervals in table 2. Each combination of dataset and interval was decoded 100 times to obtain the distribution. The boxes encompass the values between the 25th and 75th percentiles. The line and circle inside the box represent the median and mean values of the distribution, respectively. The fences limit the minimum and maximum values not considered outliers.

(jPCA projections) and the high-dimensional (PSTHs of all channels) state-spaces does not necessarily gain or lose structure over time during the planning process. In other words, it looks as if the subject is ready to execute the action early in the planning stage but is only waiting for the go cue. This result is particularly important to show that non-cued behaviour, like real-life activities, can be very well predicted with dynamical rotations.

From these observations we can not only confirm that PMd is involved in orienting motor programs in the planning phase, but we can also confidently suggest that direction-related information is better extracted from the rotational structure of neuronal trajectories than from the spiking responses of the MUA. These results are supported by several studies reporting that low-dimensional dynamics can provide as accurate or even better reconstruction of 3D movement kinematics than approaches based on direct decoding from the spike rates of the entire neuronal ensemble. [17, 21]

Another interesting observation is that decoding with jPCA projections was considerably more time-efficient than without this processing, taking an average of 500s per dataset (data not shown), and saving over 3 times the time of decoding with the information from the entire neuronal ensemble, which reaffirms the potential of jPCA projections in motor control with a BMIs.

3.2.2 Decoding movement onset

We have ascertained that the dynamics of neuronal activity in PMd rotate distinctly for different movement directions. We now want to test whether or not the

same neuronal trajectories carry information relative to when the movement should start. Some experiments have used the preparatory activity to predict the reaction time, while others have relied on different data samples labelled 'onset' or 'not onset' to decode movement onset. [22,23] Implementing the first approach with an SVM demands the discretisation of the reaction time, which has the inherent problem that two neighbouring values might belong to different classes and other two more spaced values may be grouped together. Thus, the second method seems more fitting for the purpose of comparing the rotational structure before and during motor execution. Each trial is sampled during an interval early in the preparatory (visual) phase, and in another interval immediately before the movement onset, as described in table 3. This way, each trial generates two observations.

Table 3: Intervals used in the decoding of movement onset. The column «Align» defines the event to which the starting and ending points are relative: object onset (OO) or lift of the hand (LH).

Interval	Start (ms)	End (ms)	Align
Not Onset	50	350	OO
Onset	-300	0	LH

The set of input observations are designed to sample an 'onset' and a 'not onset' interval from each trial, and, thus, the chance level for this analysis is 50%. This value was highly surpassed with either feature design (fig. 5). In particular, decoding movement onset with jPCA projections had a distinctly superior performance to that with the spike trains of the entire neuronal ensemble, reaching more than 90% correct in several data sets. Conversely, some datasets had a performance similar to that of random classification when decoding with the PSTHs of the entire neuronal ensemble.

Most channels show a very steep increase in neuronal activity during action execution comparing to the activity rates observed right after object onset, which could suggest that decoding movement onset from the trains of spike rates would be a very accurate procedure. That was, however, not the case. On the other hand, the rotational structure was not anticipated to be so distinct between the two intervals as to allow such good characterisation of the activity in that period. These results suggest that there should be some condition-invariant dynamical structure that characterises the neural state at different epochs regardless of the experimental condition. It is important to confirm in future studies that the imminence of movement initiation is, indeed, the cause of this change in dynamical organisation, and not the visual information associated with the go cue. This analysis is especially relevant when the goal are real-life applications, as there is no cue involved and thus this form of decoding would not be effective.

Once again, decoding with jPCA projection also revealed to be more time-efficient, taking about 100s to classify the observations (data not shown), a value that can be 15 times superior if using the spiking responses of the entire neuronal ensemble.

One might be inclined to conclude that jPCA projections are better suited for decoding movement onset than movement direction. But it is important to keep in mind that such comparison is not fair: in one case we are decoding a set with three labels, whereas in another case there are only two groups. It is, thus, possible that, if we sampled each condition in different epochs, the accuracy when decoding movement direction would alter. Furthermore, the number of observations used for

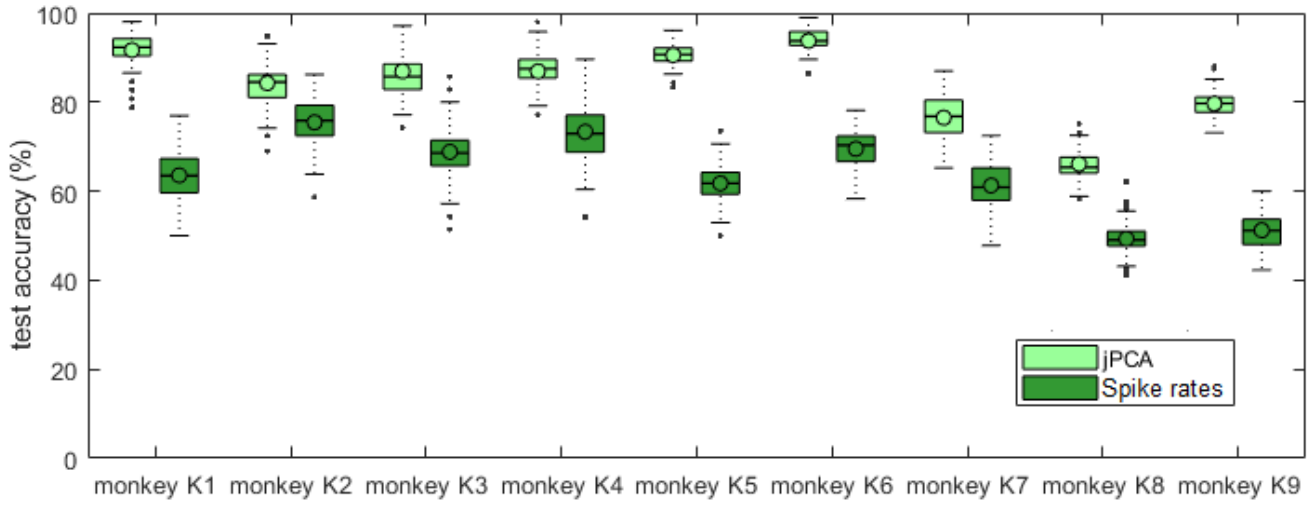

Figure 5: Accuracy of decoding movement direction with jPCA projections versus the trains of spike rates (PSTHs) of the entire neuronal ensemble. The decoding procedure was performed for datasets K1-9 for the time intervals in table 3. Each combination of interval and method was decoded 100 times to obtain the distribution for each dataset. The boxes encompass the values between the 25th and 75th percentiles. The line and circle inside the box represent the median and mean values of the distribution, respectively. The fences limit the minimum and maximum values not considered outliers.

decoding movement onset is double the amount employed to classify movement condition, which can considerably influence the accuracy of the method.

4 CONCLUSION

The difference in neuronal responses between the dorsal and ventral premotor cortices has strong implications for the development of novel BMIs controlled by the visuomotor activity of premotor neurons. Our findings represent an encouragement to research in premotor areas, as we have demonstrated that visuomotor activity encodes important information for guiding a BMI - a promising result for the rehabilitation of patients with the most varied types of motor-impairment (e.g. paralysis, locked-in syndrome, amyotrophic lateral sclerosis).

Following the dynamical perspective of neuronal activity, the fact that neuronal activity in both PMd and PMv seemed to be equally well captured by rotational dynamics in all epochs should be an argument supporting the role of both premotor areas in motor control during the whole duration of the reach-to-grasp task. This is an interesting finding that raises two very important questions: where, in the visuomotor system, do neurons start showing rotational dynamics?, and is it be possible to decode the kinematics of the motor tasks from PMv during the planning phase?

As for the first question, two hypotheses arise: either dynamical rotations in PMv are a consequence of inputs from PMd, which is supported by the FARS model [6], or this structure comes from an earlier stage of visual integration in the parietal cortex. To obtain a more definite answer, one could carry out further research in the parietal areas that provide input to the premotor cortex, i.e. area AIP for PMv and the parietal reach region (PRR) for PMd, to analyse dynamical structure or their neuronal trajectories. [5, 7] If rotational dynamics are detected not only in the parietal cortex, but also in other areas that process visual object information without intervening directly in motor planning, such as the ITC, we may argue that rotational dynamics are simply a complex epiphenomenon of visual or visuomotor information processing. [5, 6] Otherwise, this dynamical structure might be a true neuronal signature of motor planning.

Regarding the second point, it has been determined that PMv receives information about object shape, size and orientation from AIP. [6, 7, 9, 15, 24] Traditionally, this information has been thought to play a major role in grasp-related commands, such as shaping the hand for the prehension of the object. However, the existence of robust rotations in the neuronal trajectories of PMv as soon as the subject sees the object to grasp leads us to believe that this premotor area might also have valuable inputs to describe the movement direction. Further research, however, needs to validate this idea and evaluate the extent to which neuronal trajectories in PMv would be a significant addition to PMd, with respect to decoding reach direction. Despite being one of the initial goals of this project, this exploration was precluded due to technical limitations.

Decoding with jPCA projections of PMd activity revealed to be consistently less time-consuming and more accurate than using the PSTHs of the entire neuronal set. Moreover, these observations not only give further support to a dynamical interpretation of neuronal activity but also solidify the relation between rotational dynamics and motor kinematics, reinforcing the potential for controlling a motor BMI with visuomotor activity from premotor areas.

An important issue that needs to be addressed is that we investigated the functional properties of the premotor cortex in a behaving rhesus monkey, whereas our ultimate goal is to develop a novel BMI based on visuomotor activity for human use. Although the monkey brain is unquestionably the most similar to ours, evolution has provided the human brain with an elaborate neuronal network that has induced such reorganisation and expansion in premotor cortex, that studies have suggested that PMv in humans might be essential for speech processing. [25] These findings may complicate the implantation of the array in the human premotor cortex, since we are mostly interested in populations that are active during reach-to-grasp tasks.

In order to further study the limitations of controlling a BMI with premotor input, it could be interesting to increase the number of reach directions analysed in order to determine how precise gross motor commands could get under visuomotor control. Moreover, placing different sizes and shapes of objects - i.e. spheres, cubes, handles - at different distances from the subject would facilitate the study of a combination of reach kinematics with different types of grips - i.e. power grip, precision grip, key grip -, allowing a more detailed comprehension of the structure of neuronal dynamics in both premotor areas in various conditions.

Ackowledgement: This document was written and made publically available as an institutional academic requirement and as a part of the evaluation of the MSc thesis in Biomedical Engineering of the author at Instituto Superior Técnico. The work described herein was performed at the Laboratory for Neuro- and Psychophysiology of the department of Neurosciences of the Katholieke Universiteit Leuven (Leuven, Belgium), during the period of February to June 2019, under the supervision of Prof. Peter Janssen, and within the frame of the Erasmus programme. The thesis was co-supervised at Instituto Superior Técnico by Prof. João Sanches.

References

[1] M. A. Lebedev and M. A. Nicolelis, "Brain-machine interfaces: From basic science to neuroprostheses and neurorehabilitation," *Physiological reviews*, vol. 97, no. 2, pp. 767–837, 2017.

[2] C. Pandarinath, V. Gilja, C. H. Blabe, P. Nuyujukian, A. A. Sarma, B. L. Sorice, E. N. Eskandar, L. R. Hochberg, J. M. Henderson, and K. V. Shenoy, "Neural population dynamics in human motor cortex during movements in people with als," *Elife*, vol. 4, p. e07436, 2015.

[3] M. A. Dimyan and L. G. Cohen, "Neuroplasticity in the context of motor rehabilitation after stroke," *Nature Reviews Neurology*, vol. 7, no. 2, p. 76, 2011.

[4] S. staff. (2009) Visuomotor skills. [Online]. Available: https://www.aboutkidshealth.ca/Article?contentid=1879&language=English

[5] P. Janssen, B.-E. Verhoef, and E. Premereur, "Functional interactions between the macaque dorsal and ventral visual pathways during three-dimensional object vision," *Cortex*, vol. 98, pp. 218–227, 2018.

[6] A. H. Fagg and M. A. Arbib, "Modeling parietal–premotor interactions in primate control of grasping," *Neural Networks*, vol. 11, no. 7-8, pp. 1277–1303, 1998.

[7] E. Oztop, "Modeling the mirror: grasp learning and action recognition," Ph.D. dissertation, University of Southern California, 2002.

[8] G. Rizzolatti, R. Camarda, L. Fogassi, M. Gentilucci, G. Luppino, and M. Matelli, "Functional organization of inferior area 6 in the macaque monkey," *Experimental brain research*, vol. 71, no. 3, pp. 491–507, 1988.

[9] A. Murata, W. Wen, and H. Asama, "The body and objects represented in the ventral stream of the parieto-premotor network," *Neuroscience research*, vol. 104, pp. 4–15, 2016.

[10] E. Hoshi and J. Tanji, "Differential involvement of neurons in the dorsal and ventral premotor cortex during processing of visual signals for action planning," *Journal of neurophysiology*, vol. 95, no. 6, pp. 3596–3616, 2006.

[11] M. J. Grol, J. Majdandzi, K. E. Stephan, L. Verhagen, H. C. Dijkerman, H. Bekkering, F. A. Verstraten, and I. Toni, "Parieto-frontal connectivity during visually guided grasping," *Journal of Neuroscience*, vol. 27, no. 44, pp. 11 877–11 887, 2007.

[12] P. Cisek and J. F. Kalaska, "Neural correlates of reaching decisions in dorsal premotor cortex: specification of multiple direction choices and final selection of action," *Neuron*, vol. 45, no. 5, pp. 801–814, 2005.

[13] K. Takahashi, M. D. Best, N. Huh, K. A. Brown, A. A. Tobaa, and N. G. Hatsopoulos, "Encoding of both reaching and grasping kinematics in dorsal and ventral premotor cortices," *Journal of Neuroscience*, vol. 37, no. 7, pp. 1733–1746, 2017.

[14] E. R. Kandel, J. H. Schwartz, T. M. Jessel, S. A. Siegelbaum, and A. J. Hudspeth, *Principles of Neural Science, Fifth Edition*. The McGraw-Hill Companies, Inc, 2013, vol. 2.

[15] P. A. Chouinard, "Different roles of pmv and pmd during object lifting," *Journal of Neuroscience*, vol. 26, no. 24, pp. 6397–6398, 2006.

[16] M. M. Churchland, J. P. Cunningham, M. T. Kaufman, J. D. Foster, P. Nuyujukian, S. I. Ryu, and K. V. Shenoy, "Neural population dynamics during reaching," *Nature*, vol. 487, no. 7405, p. 51, 2012.

[17] J. A. Michaels, B. Dann, and H. Scherberger, "Neural population dynamics during reaching are better explained by a dynamical system than representational tuning," *PLoS computational biology*, vol. 12, no. 11, p. e1005175, 2016.

[18] D. Sussillo, M. M. Churchland, M. T. Kaufman, and K. V. Shenoy, "A neural network that finds a naturalistic solution for the production of muscle activity," *Nature neuroscience*, vol. 18, no. 7, p. 1025, 2015.

[19] A. H. Lara, J. P. Cunningham, and M. M. Churchland, "Different population dynamics in the supplementary motor area and motor cortex during reaching," *Nature communications*, vol. 9, no. 1, p. 2754, 2018.

[20] C. Pandarinath, D. J. OâĂŹShea, J. Collins, R. Jozefowicz, S. D. Stavisky, J. C. Kao, E. M. Trautmann, M. T. Kaufman, S. I. Ryu, L. R. Hochberg *et al.*, "Inferring single-trial neural population dynamics using sequential auto-encoders," *Nature methods*, p. 1, 2018.

[21] M. Aghagolzadeh and W. Truccolo, "Inference and decoding of motor cortex low-dimensional dynamics via latent state-space models," *IEEE Transactions on Neural Systems and Rehabilitation Engineering*, vol. 24, no. 2, pp. 272–282, 2015.

[22] K. V. Shenoy, M. Sahani, and M. M. Churchland, "Cortical control of arm movements: a dynamical systems perspective," *Annual review of neuroscience*, vol. 36, pp. 337–359, 2013.

[23] Z. Wang, A. Gunduz, P. Brunner, A. L. Ritaccio, Q. Ji, and G. Schalk, "Decoding onset and direction of movements using electrocorticographic (ecog) signals in humans," *Frontiers in neuroengineering*, vol. 5, p. 15, 2012.

[24] M. Umiltà, I. Intskirveli, F. Grammont, M. Rochat, F. Caruana, A. Jezzini, V. Gallese, G. Rizzolatti *et al.*, "When pliers become fingers in the monkey motor system," *Proceedings of the National Academy of Sciences*, vol. 105, no. 6, pp. 2209–2213, 2008.

[25] I. G. Meister, S. M. Wilson, C. Deblieck, A. D. Wu, and M. Iacoboni, "The essential role of premotor cortex in speech perception," *Current Biology*, vol. 17, no. 19, pp. 1692–1696, 2007.